International Journal of Cardiology 278 (2019) 114–119

Contents lists available at ScienceDirect

International Journal of Cardiology

journal homepage: www.elsevier.com/locate/ijcard

Left atrial scarring and conduction velocity dynamics: Rate dependent conduction slowing predicts sites of localized reentrant atrial tachycardias

S. Honarbakhsh [1], R.J. Schilling [1], M. Orini [1], R. Providencia [1], M. Finlay [1], E. Keating [1], P.D. Lambiase [1], A. Chow [1], M.J. Earley [1], S. Sporton [1], R.J. Hunter *,[1]

Barts Heart Centre, Barts Health NHS Trust, London, United Kingdom

ARTICLE INFO

Article history:
Received 19 September 2018
Received in revised form 16 October 2018
Accepted 22 October 2018
Available online 24 October 2018

Keywords:
Conduction velocity
Conduction velocity heterogeneity
Atrial tachycardia
Structural remodeling
Catheter ablation

ABSTRACT

Background: Low voltage zones (LVZs) are associated with conduction velocity (CV) slowing. Rate-dependent CV slowing may play a role in reentry mechanisms.
Methods: Patients undergoing catheter ablation for AT were enrolled. Aim was to assess the relationship between rate-dependent CV slowing and sites of localized reentrant atrial tachycardias (AT). On a bipolar voltage map regions were defined as non-LVZs [≥0.5 mV], LVZs [0.2–0.5 mV] and very-LVZs [<0.2 mV]. Unipolar electrograms were recorded with a 64-pole basket catheter during uninterrupted atrial pacing at four pacing intervals (PIs) during sinus rhythm. CVs were measured between pole pairs along the wavefront path. Sites of rate-dependent CV slowing were defined as exhibiting a reduction in CV between PI = 600 ms and 250 ms of ≥20% more than the mean CV reduction seen between these PIs for that voltage zone. Rate-dependent CV slowing sites were correlated to sites of localized reentrant ATs as confirmed with conventional mapping, entrainment and response to ablation.
Results: Eighteen patients were included (63 ± 10 years). Mean CV at 600 ms was 1.53 ± 0.19 m/s in non-LVZs, 1.14 ± 0.15 m/s in LVZs, and 0.73 ± 0.13 m/s in very-LVZs respectively ($p < 0.001$). Rate-dependent CV slowing sites were predominantly in LVZs [0.2–0.5 mV] (74.4 ± 10.3%; $p < 0.001$). Localized reentrant ATs were mapped to these sites in 81.8% of cases (sensitivity 81.8%, 95% CI 48.2–97.9% and specificity 83.9%, 95% CI 81.8–86.0%). Macro-reentrant or focal ATs were not mapped to sites of rate-dependent CV slowing.
Conclusions: Rate-dependent CV slowing sites are predominantly confined to LVZs [0.2–0.5 mV] and the resultant CV heterogeneity may promote reentry mechanisms. These may represent a novel adjunctive target for AT ablation.

1. Introduction

Left atrial (LA) structural remodeling in the form of low voltage zones (LVZs) on bipolar voltage maps or late gadolinium enhancement on cardiac MRI is associated with lower local conduction velocity (CV) compared to healthy tissue [1–3]. Changes in CV with rate, i.e. CV dynamics, are also influenced by the presence of structural remodeling whereby the rate-adaptation of CV is smaller and occurs at longer pacing intervals (PIs) [4,5]. These differences may contribute to reentry [5,6]. The presence of sites with marked CV slowing with increasing rate, i.e. rate-dependent CV slowing sites, are associated with the ability to induce AF [7] and correspond to sites of reentry initiation at AF onset [8].

Atrial tachycardias (AT) are a significant problem, particularly following previous AF ablation. The atrial substrate is complex in this setting, involving both heterogeneous structural remodeling with additional scarring due to ablation which may be widespread and extensive. In this scenario there can often be multiple AT circuits and mapping can be hindered by difficulty detecting and timing low voltage fractionated electrograms. AT in this setting may rely on a zone of slow conduction [9], or simply revolve around a central core of dense scar [10]. No attempt has ever been made to understand CV dynamics in the complex substrate of patients with ATs. We hypothesized that in a mixed group of patients with heterogeneous atrial scarring due to structural remodeling and/or previous ablation, abnormalities of CV dynamics could be defined that would predict sites of localized reentry. We aimed to define clinically relevant perturbations of CV dynamics in a practical way that might facilitate future

* Corresponding author at: Barts Heart Centre, Barts Health NHS Trust, W.Smithfield, EC1A 7BE, United Kingdom.
E-mail address: ross.hunter@bartshealth.nhs.uk (R.J. Hunter).
[1] This author takes responsibility for all aspects of the reliability and freedom from bias of the data presented and their discussed interpretation.

https://doi.org/10.1016/j.ijcard.2018.10.072
0167-5273/

development of a substrate modification strategy as an adjunct to conventional mapping and ablation for AT.

2. Method

2.1. Study design

Patients undergoing catheter ablation for AT (de-novo or following AF ablation) were prospectively included in this study. All patients were in sinus rhythm at the start of the case (following prior DC cardioversion ± anti-arrhythmic drugs). All patients provided informed consent for their participation in this study. This study was approved by the UK Research Ethics Committee (London - Bloomsbury Research Ethics Committee, 16/LO/1379).

2.2. Electrophysiological mapping

Mapping was performed with the CARTOFINDER mapping system (CARTO, Biosense Webster, Inc., CA) ([11–13], Supplemental Method).

LA geometry and a high-density bipolar voltage map were created in sinus rhythm using a PentaRay® NAV catheter with 2-6-2 mm electrode spacing (Biosense Webster, Inc., CA) (Supplemental Method). Non-LVZs were defined as sites with a bipolar voltage of [≥0.5 mV], LVZ was defined as [0.2–0.5 mV], and very LVZ (vLVZ) was defined as [<0.2 mV] [14–16]. Bipolar voltages obtained at the pulmonary veins (PVs), mitral valve annulus and LA appendage (LAA) were excluded to allow for a mean bipolar voltage of the LA body only.

A 64-pole basket catheter (Constellation, Boston Scientific Ltd., Natick, MA or FIRMap, Abbott, CA, USA) was used to record unipolar signals and was positioned to achieve optimal coverage [17] (Supplemental Method).

2.3. Pacing procedure

Uninterrupted atrial pacing with the ablation catheter was performed in sinus rhythm from four sites in the LA: endocardial proximal and distal coronary sinus (CS), LA roof and LAA. This method was adapted from a previously published method [7]. This was to ensure that wavefront propagations in different directions were achieved. At each site pacing was performed at four pacing intervals (PIs) (600 ms, 450 ms, 300 ms, 250 ms) for 30 s each. During the 30-second unipolar electrogram recording, a location point was also taken on CARTO3 to obtain 3D coordinates for each pole.

2.4. Local CVs

Unipolar electrograms, electrode location and left atrial geometry data were imported into MATLAB (MathWorks, MA) and utilizing an automated custom written script each basket catheter electrode was paired to a neighboring electrode within a known geodesic distance. CV was assessed over a distance of 5–30 mm with electrode pairs closer or further apart than this excluded from the analysis. Following this, only electrode pairs with adequate contact were included. Contact was defined as per previous study [17,18] whereby electrodes that were <10 mm from the geometry were defined as being in contact. The electrograms were then reviewed on the electrodes that were within 10 mm of the geometry to ensure that electrograms were adequate for analysis. Following this, electrode pair position was verified on the LA geometry. CV was measured only between electrode pairs oriented parallel to the direction of wavefront propagation as determined by manual review of propagation maps on CARTOFINDER, which has been previously validated in terms of demonstrating wavefront propagation [13]. Further to this, the CARTOFINDER system has shown to accurately annotate atrial signals without inappropriate annotation on far-field ventricular signals [12,13]. This process was conducted for all four pacing sites and PIs. To determine the CV, firstly the local activation time was calculated as the interval between the pacing spike and the steepest descent (peak negative dv/dt) in the unipolar electrogram. The last beat of the 30-second recording was used for this analysis. The CV between each electrode pair was defined as the geodesic distance between the electrodes divided by the activation time difference. CVs were expressed in m/s. Pairs that had an activation time difference of <1 ms at 600 ms PI were excluded as sites of simultaneous activation.

An automated custom written script was used to ensure consistency between all CV measurements in all patients included in this study and to minimize the effect of human error. However, to assess the accuracy of the automated script we compared 50 CV measurements obtained manually with that obtained using the automated script.

2.5. CV heterogeneity and rate-dependent CV slowing

Using an automated MATLAB custom written script the position of the electrode pairs that were included in the analysis, was projected onto the LA geometry. The position of the bipolar voltage points taken with the PentaRay catheter was also projected on the same LA geometry. These points were considered within a 5 mm band between the electrodes from which CV was assessed. The mean of these was taken as the local bipolar voltage along the path between each electrode pair (Supplemental Fig. 1).

Areas were then subdivided into non-LVZs, LVZs or vLVZs according to the mean bipolar voltage along the path. CV at each PI was compared in these three areas. Heterogeneity in CV dynamics was examined in these zones and sites of rate-dependent CV slowing were identified. These were defined as zones exhibiting a reduction in CV between PI = 600 ms and PI = 250 ms of ≥20% more than the mean CV reduction seen between these PIs for that voltage zone.

2.6. CV and ATs

Arrhythmia was induced following the study protocol by burst atrial pacing from the CS starting at PI of 400 ms, with a 10 ms decrement until either arrhythmia was induced or reaching 200 ms. If this did not induce the arrhythmia then this was repeated from elsewhere in the atria. ATs were mapped using the CARTOFINDER system as described previously [13]. The AT mechanisms were confirmed with conventional local activation time (LAT) maps, entrainment and ablation response. Locations of reentrant ATs were correlated to sites of rate-dependent CV slowing. Following ablation of AT, attempts were made to induce further AT which were also mapped and ablated. The clinical end-point was non-inducibility of AT.

We adopted a classification of ATs proposed previously [19]. In brief, tachycardias were defined as (i) focal tachycardias which mapped to a discrete earliest point, (ii) macro-reentry whereby the entire cycle length (CL) can be mapped surrounding an anatomical obstacle, or (iii) localized reentry whereby the CL can be mapped to an area of <2 cm diameter.

2.7. Statistical analysis

This was performed using SPSS (IBM SPSS Statistics, Version 25 IBM Corp, Armonk, NY, USA). Continuous variables are displayed as mean ± standard deviation (SD). Categorical variables are presented as a number and percentage. Chi-square was used for the comparison of nominal variables. The Student *t*-test, or its non-parametric equivalent, Mann-Whitney when appropriate, was used for comparison of continuous variables. ROC curves were performed to determine the association between different parameters and AT sites. *p*-Values <0.05 were regarded as significant.

3. Results

Eighteen patients were included (Supplemental Table 1).

3.1. CV and bipolar voltage

14,785 bipolar voltage points were taken with an average of 821 ± 201 points per patient, of which an average of 402 ± 181 points were <0.5 mV (49 ± 22%). The mean bipolar voltage was 0.43 ± 0.16 mV. LVZs occurred as islands or plaques each one covering a minimum of 10% of the LA surface (27 ± 16%). LVZs predominantly affected the anterior (42%) and posterior wall (23%). The remainder included the septum (16%), lateral wall (12%) and roof (7%).

CV was determined over a total of 4922 electrode pairs with a mean of 63.3 ± 16.8 pairs for each activation sequence in each patient. The mean CV at PI of 600 ms at non-LVZ [≥0.5 mV] was 1.53 ± 0.19 m/s, 1.14 ± 0.15 m/s at LVZ [0.2–0.5 mV] and 0.73 ± 0.13 m/s at vLVZ [<0.2 mV]. There was a strong correlation between mean CV and mean bipolar voltage ($r_s = 0.99$, $p < 0.001$; Supplemental Fig. 2A) and proportion of LVZs ($r_s = -0.97$, $p < 0.001$; Supplemental Fig. 2B).

There was a 98% consistency between the 50 CV measurements obtained using either manual calculations or the automated custom written script.

3.2. CV dynamics and bipolar voltage

The CV change over the four PIs was different in the three voltage zones (Fig. 1). In non-LVZs [≥0.5 mV] the CV remained relatively stable until a significant reduction was seen in the CV between PIs 300 and 250 ms (0.588 ± 0.082 m/s; $p < 0.001$). In LVZs [0.2–0.5 mV] the reduction in CV was continuous and progressive across reducing PIs, with a significant reduction in the CV across all four PIs (0.094 ± 0.06 m/s; $p < 0.001$). In vLVZs [<0.2 mV] the CV curves remained relatively flat across the four PIs with a total reduction in CV between 600 and 250 ms of 0.01 ± 0.008 m/s ($p = 0.45$).

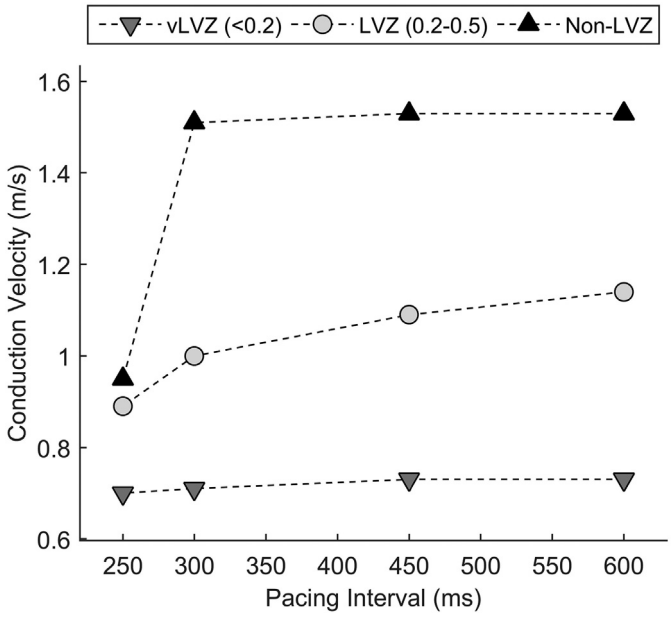

Fig. 1. Demonstrates the change in CV over the four PIs in non-LVZs [≥0.5 mV] (black triangle), LVZs [0.2–0.5 mV] (light grey circle) and vLVZs [<0.2 mV] (dark grey triangle).

3.3. Relationship between rate-dependent CV slowing sites and bipolar voltage

For each pacing location, a mean of 11.4 ± 3.8 rate-dependent CV slowing sites were observed per patient (22.7 ± 6.0% of sites sampled). The proportion of rate-dependent CV slowing sites identified per patient was not dependent on whether the patient was on an anti-arrhythmic drug or not (11.0 ± 4.3 vs. 11.6 ± 3.4; $p = 0.76$). In relation to voltage zones 74.4 ± 10.3% of rate-dependent CV slowing sites were found in LVZs [0.2–0.5 mV] versus 25.6 ± 10.2% in non-LVZs [>0.5 mV] and 0 ± 0% in vLVZ [<0.2 mV]; ($p < 0.001$; Fig. 2A). The percentage of measurements with rate-dependent CV slowing was 17.2 ± 3.1% for LVZ [0.2–0.5 mV], 6.1 ± 3.4% in non-LVZs [>0.5 mV] and 0 ± 0% for vLVZ [<0.2 mV] ($p < 0.001$) (Fig. 2B). Further to this, rate-dependent CV slowing sites were more prevalent in patients with a lower mean bipolar voltage ($r_s = -0.96, p < 0.001$). They were also more commonly mapped to the anterior (44%) and posterior (20%) wall, which correlated to sites where LVZs were more frequent.

The rate-dependent CV slowing sites in LVZs were all in the LVZ range [0.2–0.5 mV] and showed progressive decrease in CV over all four PIs (mean decrease in CV of 0.13 ± 0.03 m/s for each PI) resulting in broader curves (Fig. 2C). The reduction in CV between PI of 600 and 250 ms at these sites was 0.38 ± 0.05 m/s or a reduction in CV of 37.7 ± 0.03%. Since this reduction was progressive across PI in LVZ [0.2–0.5 mV], this equated to a reduction in CV between PI 600 and 300 ms of 0.22 ± 0.03 m/s at these sites, or a reduction of 21.9 ± 0.02%.

However, rate-dependent CV slowing sites in non-LVZs behaved differently, with the greatest decrease in CV seen between PI of 300 and 250 ms (mean decrease in CV of 0.67 ± 0.12 m/s; $p = 0.001$) with minimal change at longer PIs, resulting in a steeper curve (Fig. 2C).

3.4. Relationship between rate-dependent CV slowing sites and ATs

In the 18 AT patients, 23 ATs were mapped and ablated (Supplemental Table 2). Of these, 12 were non-macro-reentrant ATs mapped to the LA in 10 patients and out of these 11 were sustained by a localized reentry mechanism and 1 was focal. Out of the 11 localized reentrant ATs 5 (45.5%) correlated to sites of previous AF ablation (2 at sites of previous roof line and 3 at sites of previous CFAE ablation).

Of the 11 LA localized reentrant ATs, 10 were mapped to sites of LVZ [0.2–0.5 mV] (91.9%) with a mean bipolar voltage of 0.28 ± 0.11 mV and 1 was mapped to a non-LVZ. Nine were mapped to sites of rate-dependent CV slowing (81.8%) in LVZs [0.2–0.5 mV] (Fig. 3A–C). In the one AT patient thought to have a truly focal mechanism this was mapped to an area of non-LVZs which was not associated with rate-dependent CV slowing.

LVZs predicted sites of localized reentrant AT with high sensitivity (90.9%, 95% CI 58.7–99.8%) but low specificity (36.1%, 95% CI 32.8–39.4%). Rate-dependent CV slowing sites showed a sensitivity and specificity of 81.8% (95% CI 48.2–97.9%) and 83.9% (95% CI 81.8–86.0%) for predicting sites of localized reentry.

Heterogeneity in bipolar voltage within LVZs and the surface area of a LVZ were not strong predictors of localized reentry in LVZs. CV during pacing at 600 ms was also not a strong predictor of localized reentry in LVZs. The percentage of CV measurements within an area of scar exhibiting rate-dependent CV slowing and the percentage of CV change in these rate-dependent CV slowing sites was the strongest predictor of localized reentry within LVZs (Table 1).

3.5. Follow-up data

During a follow-up of 16.6 ± 2.5 months none of the patients had recurrence of AT.

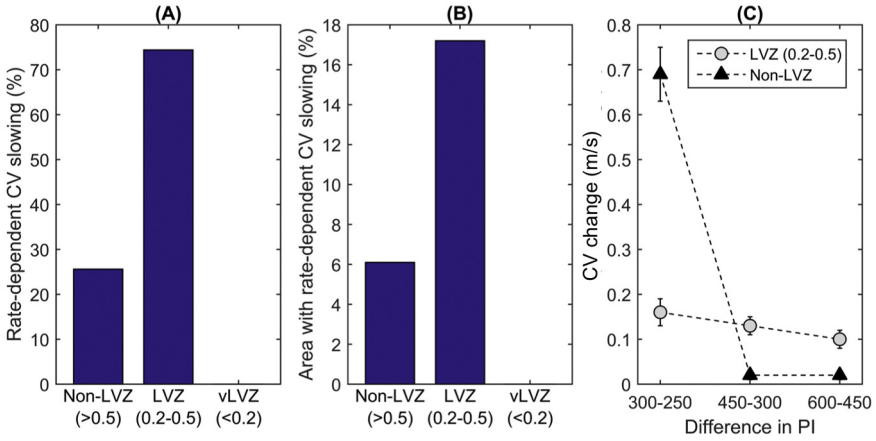

Fig. 2. A–C (A) Bar chart shows the percentage of the rate-dependent CV slowing sites in non-LVZs [≥0.5 mV], LVZs [0.2–0.5 mV] and vLVZs [<0.2 mV] and (B) the proportion of non-LVZs [≥0.5 mV], LVZs [0.2–0.5 mV] and vLVZs [<0.2 mV] demonstrating rate-dependent CV slowing. (C) Demonstrates the CV reduction between the four PIs (600–450 ms, 450–300 ms and 300–250 ms) in rate-dependent CV slowing sites in non-LVZs [≥0.5 mV] and LVZs [0.2–0.5 mV].

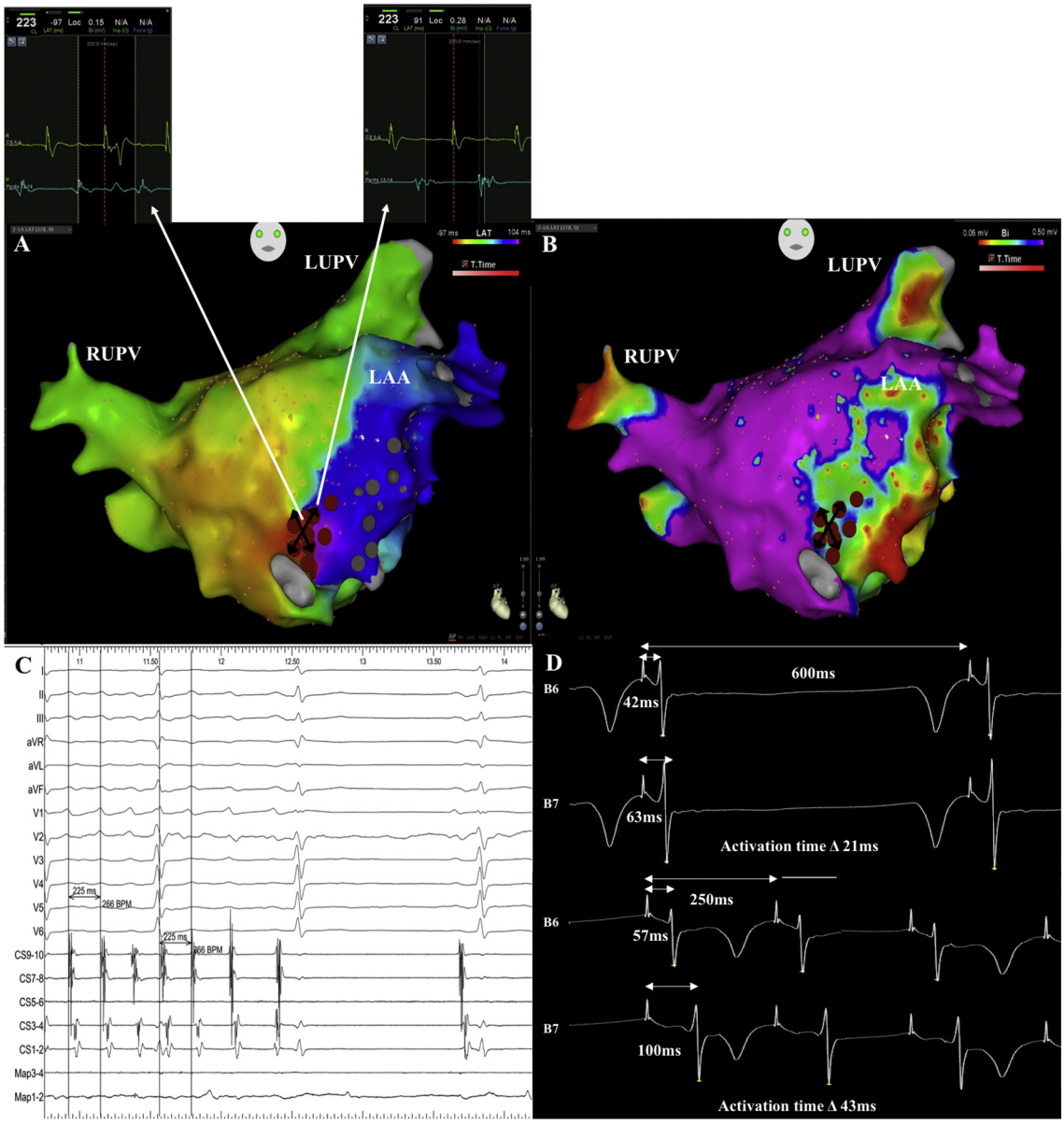

Fig. 3. A–C (A) Conventional activation map (anterior-posterior view) of a localized reentrant AT mapped to the low anterior wall of the LA with the electrograms used to time in relation to the reference electrode. (B) Bipolar voltage map demonstrating LVZ at the site of the localized reentrant AT. (C) Electrogram recordings demonstrating slowing of AT followed by termination to sinus rhythm on ablation (red circles on panel A and B show ablation lesions). (D) Electrograms demonstrating the rate-dependent slowing site mapped to the LVZ (highlighted by the black arrows on panel A and B) that corresponds to the site of the localized reentrant AT. The activation time difference between electrodes B6 and B7 on the basket catheter, that transects this area, during pacing in sinus rhythm increased by 100% when pacing at a PI of 250 ms from 600 ms. LUPV- left upper pulmonary vein. RUPV- right upper pulmonary vein. LAA- left atrial appendage.

4. Discussion

This is the first study to comprehensively investigate CV dynamics in the complex substrate of patients with AT. The CVs were proportional to voltage irrespective of the mixed etiology of the scarring. The CV dynamic curves were different across areas with different degrees of scarring: healthy tissue had CV slowing only at PI of 250 ms, LVZs [0.2–0.5 mV] had the curve shifted to the right showing significant slowing from 400 ms, whereas vLVZs [<0.2 mV] was very slow at 600 ms and remained flat with little further slowing. Almost all localized reentrant AT were found in LVZs [0.2–0.5 mV], however, these were sensitive for sites of localized reentry but not specific. Sites of rate-dependent CV slowing were both sensitive and specific for sites of localized reentry causing AT. These rate-dependent CV slowing sites in LVZ [0.2–0.5 mV] were evident when pacing at 300 ms potentially allowing them to be identified with an abbreviated protocol by pacing at only 2 PIs (600 ms and 300 ms).

ATs are a significant clinical problem and encountered frequently following AF ablation. Attempts to target drivers in AF have often reduced the proportion of patients with recurrent AF but often at the expense of more patients with recurrent AT instead [20,21]. AT due to localized re-entry is a particular problem in this context with scarring caused by both remodeling and ablation lesions. This may allow slow conduction zones, or simply create a central core of dense scar around which wavefronts can revolve [9,10]. There is currently interest in targeting LVZs for AF as this may represent sites for reentry formation [22–24]. This could be considered for AT, but areas of scarring are likely to be widespread. The feasibility of examining CV dynamics in the scarred LA of patients with AT has not been investigated previously and this may identify potential targets for a conservative substrate ablation strategy.

Table 1
The value of different factors in predicting drivers in AT.

Each LVZ island	AUC	*p*-Value	95% CI	Optimal cutoff value	Sensitivity	Specificity
Surface area cm^2	0.51	0.34	0.34–0.69	3.2	0.74	0.64
Mean bipolar voltage mV	0.84	<0.001	0.72–0.96	0.30	0.90	0.65
SD of mean bipolar voltage mV	0.50	0.99	0.32–0.68	0.14	0.54	0.52
CV[a] at 600 ms m/s	0.75	0.002	0.64–0.94	1.21	0.74	0.74
% CV measurements demonstrating RD[b] CV slowing	0.84	<0.001	0.71–0.98	19.1	0.82	0.93
% CV change in RD CV slowing sites	0.87	<0.001	0.74–0.98	56.3	0.84	0.94

[a] CV- conduction velocity.
[b] RD- rate-dependent.

A majority of the patients in this study had undergone prior ablation for AF, although none had panoramic mapping of drivers during these procedures. Of the 11 localized reentrant ATs 5 corresponded to sites of prior ablation. These sites may therefore relate to iatrogenic scarring, although it has been suggested that the mechanisms of some AT may overlap with those of drivers initially present in AF [25,26].

4.1. CV and bipolar voltage

LVZ were clustered in relatively large regions or 'islands' rather than scattered throughout the myocardium. The focal nature of this remodeling process has been observed previously [16,27,28], and enabled an accurate assessment of CV dynamics within these zones. The strong correlation between mean CV and both mean bipolar voltage and the proportion of LVZs demonstrates a strong link between structural and electrical remodeling.

4.2. CV dynamics and bipolar voltage

The CV reduction over the four PIs differed markedly amongst the three voltage zones. In non-LVZs [≥0.5 mV] the CV change was significant only between PI of 300 and 250 ms whereby a steep reduction in CV was seen consistent with that seen in healthy myocardial tissue [5]. CV dynamics were different in LVZs and furthermore differed significantly between LVZs [0.2–0.5 mV] and vLVZs [<0.2 mV]. Whilst in LVZs [0.2–0.5 mV] CV started to reduce at a longer PI resulting in broad curves, in vLVZs [<0.2 mV] there was minimal rate-adaptation seen with reducing PI resulting in flat CV curves. With structural remodeling there is replacement of myocardial tissue by fibrosis [8,14], alteration in gap junction communication [29] and coupling of myocytes with fibroblasts [30]. These phenomena may contribute to the slowing of conduction and altered CV dynamics curves seen in LVZs.

4.3. Relationship between rate-dependent CV slowing sites and bipolar voltage

There were a greater percentage of rate-dependent CV slowing sites in LVZs than non-LVZs with a direct correlation between the proportion of LVZs and the number of rate-dependent CV slowing sites identified. However, rate-dependent CV slowing sites were limited to LVZs [0.2–0.5 mV] with no sites identified in vLVZs [<0.2 mV]. Thereby all LVZs do not play an equal mechanistic importance in CV dynamics. Rate-dependent CV slowing sites being limited to LVZs [0.2–0.5 mV] is potentially as a result of the tissue being healthy enough to be capable of near normal CV at longer PIs (600 ms), but is abnormal enough to reduce CV significantly with shorter PIs (<600 ms). In contrast, the tissue in vLVZs <0.2 mV is markedly diseased and as a result the CV at 600 ms is already very slow and there is no rate-adaptation feasible resulting in no conduction reserve.

4.4. Relationship between rate-dependent CV slowing sites and ATs

The majority of the non-macro-reentrant ATs had a localized reentry mechanism rather than a focal mechanism, which is consistent with other reports in patients post AF ablation [31]. These data suggest that rate-dependent CV slowing plays an important role in these reentry mechanisms, since a majority of the localized reentrant ATs were mapped to these sites. The focal AT did not correlate with low voltage, slow CV or rate-dependent CV slowing, and hence other mechanisms are likely responsible for truly focal AT for example an automatic focus.

Interestingly rate-dependent CV slowing sites were also identified in non-LVZs. It is unclear why areas with healthy endocardial voltage also demonstrate CV heterogeneity. As bipolar voltage map only allows the assessment of fibrosis/scar at an endocardial level it is possible that the presence of sub-endocardial or epicardial fibrosis results in the CV heterogeneity seen. The pattern of rate-dependent CV slowing at non-LVZs [≥0.5 mV] was different to that seen at LVZs [0.2–0.5 mV] whereby the curves were steeper with the greatest change in CV seen between PI 350 and 250 ms whilst at LVZs [0.2–0.5 mV] the change in CV was almost equally distributed across all four PIs resulting in broader CV dynamic curves. This difference can potentially explain the lack of mechanistic importance of the rate-dependent CV slowing sites mapped to non-LVZs [≥0.5 mV] as supported by no localized reentrant ATs having been mapped to these sites. It has been shown that sites with a broad CV dynamics curve have an alteration in activation vector and arcing with accelerated rates which may reflect rate-dependent conduction block in certain directions [7] which may promote initiation of reentry [32]. Further to this, the lack of mechanistic importance of rate-dependent CV slowing in non-LVZs could be because the fibrosis/scar needs to be transmural to effectively promote reentry.

The data from this feasibility study outlines a potential rationale for a substrate modification strategy as an adjunct to conventional mapping and ablation for AT. Discerning sites with rate-dependent CV slowing appears feasible, and targeting such areas only in LVZs [0.2–0.5 mV] would be conservative in terms of the amount of ablation required and may reduce the potential for subsequent localized reentry. These data suggest that a pragmatic protocol might be to focus assessment of LVZs [0.2–0.5 mV], that pacing from a single site is sufficient, and that pacing at only 2 PIs (600 ms and 300 ms) ought to be sufficient looking for a reduction in CV of 0.22 ± 0.03 m/s or 21.9 ± 0.02%. A more focused pacing protocol focusing on areas of low voltage may allow assessment of CV using other multipolar catheters. High density mapping of such areas may offer further insights into CV dynamics in these regions. It is possible that imaging of scar using techniques such as MRI may help to characterize such sites and facilitate their identification.

4.5. Limitations

One of the study limitations is the small patient numbers. This was overcome to some extent through assessing CV between >4000 electrode pairs to allow regional analysis of multiple LVZs in each patient. LA coverage achieved with the basket catheter is limited and as a result the number of rate-dependent CV slowing sites is inevitably underestimated. There was no apparent effect of the pacing site on the CV measured. However, the impact of fiber orientation and anisotropic effect on CV was not directly assessed in this study. Assessment of CV over much smaller areas and use of novel methods to assess fiber orientation [33] may allow this to be explored further.

5. Conclusions

Despite the heterogeneous nature of LA scarring in patients with AT and the practical limitations to assessing CV in-vivo, there is a clear relationship between voltage and CV with distinct patterns in CV dynamics at different voltage zones. Localized reentrant AT occurred almost exclusively in LVZs [0.2–0.5 mV] which were sensitive but not specific in predicting these sites. Rate-dependent CV slowing sites was both sensitive and specific for predicting reentry sites. It may be practical to identify these sites with relatively simple and pragmatic pacing protocols. Rate-dependent CV slowing sites in LVZs [0.2–0.5 mV] may represent a novel potential target for patients with AT.

Supplementary data to this article can be found online at https://doi.org/10.1016/j.ijcard.2018.10.072.

Disclosures

Prof. Schilling has received speaker and travel grants from Biosense Webster and research grants from Biosense Webster and Boston Scientific. Dr. Hunter has received travel grants from Biosense Webster and Medtronic. Prof Lambiase receives educational and research grants from Boston Scientific.

Funding

Project Grant from the British Heart Foundation (PG/16/10/32016) funded this work.

References

[1] K. Miyamoto, T. Tsuchiya, S. Narita, T. Yamaguchi, Y. Nagamoto, S. Ando, K. Hayashida, Y. Tanioka, N. Takahashi, Bipolar electrogram amplitudes in the left atrium are related to local conduction velocity in patients with atrial fibrillation, Europace 11 (2009) 1597–1605.
[2] J.F. Viles-Gonzalez, A. Gomes, M.A. Miller, S.R. Dukkipati, J.S. Koruth, C. Eggert, J. Coffey, V.Y. Reddy, A. d'Avilla, Areas with complex fractionated atrial electrograms recorded after pulmonary vein isolation represent normal voltage and conduction velocity in sinus rhythm, Europace 15 (2013) 339–346.
[3] K. Fukumoto, M. Habibi, E.G. Ipek, et al., Association of local left atrial conduction velocity with late gadolinium enhancement on cardiac magnetic resonance in patients with atrial fibrillation, Circ. Arrhythm. Electrophysiol. 9 (2016), e002897.
[4] M.L. Koller, S.K. Maier, A.R. Gelzer, W.R. Bauer, M. Meesmann, R.F. Gilmour Jr., Altered dynamics of action potential restitution and alternans in humans with structural heart disease, Circulation 112 (2005) 1542–1548.
[5] W. Bian, L. Tung, Structure-related initiation of re-entry by rapid pacing in monolayers of cardiac cells, Circ. Res. 98 (2006) e29–e38.
[6] Z. Qu, A. Garfinkel, P.S. Chen, J.N. Weiss, Mechanisms of discordant alternans and induction of re-entry in stimulated cardiac tissue, Circulation 102 (2000) 1664–1670.
[7] G.G. Lalani, A. Schricker, M. Gibson, A. Rostamian, D.E. Krummen, S.M. Narayan, Atrial conduction slows immediately before the onset of human atrial fibrillation: a bi-atrial contact mapping study of transitions to atrial fibrillation, J. Am. Coll. Cardiol. 59 (2012) 595–606.
[8] A.A. Schricker, G.G. Lalani, D.E. Krummen, W.J. Rappel, S.M. Narayan, Human atrial fibrillation initiates via organized rather than disorganized mechanisms, Circ. Arrhythm. Electrophysiol. 7 (2014) 816–824.
[9] V. Luther, N. Qureshi, P.B. Lim, M. Koa-Wing, S. Jamil-Copley, F.S. Ng, Z. Whinnett, D.W. Davies, N.S. Peters, P. Kanagaratnam, N. Linton, Isthmus sites identified by Ripple Mapping are usually anatomically stable: a novel method to guide atrial substrate ablation? J. Cardiovasc. Electrophysiol. 29 (2018) 404–411.
[10] V. Luther, M. Sikkel, N. Bennet, et al., Visualizing localized reentry with ultra-high density mapping in iatrogenic atrial tachycardia: beware of pseudo-reentry, Circ. Arrhythm. Electrophysiol. 10 (2017) (pii: e004724).
[11] E.G. Daoud, Z. Zeidan, J.D. Hummel, R. Weiss, M. Houmsse, R. Augostini, S.J. Kalbfleisch, Identification of repetitive activation patterns using novel computational analysis of multielectrode recordings during atrial fibrillation and flutter in humans, JACC Clin. Electrophysiol. 3 (2017) 207–216.
[12] S. Honarbakhsh, R.J. Schilling, G. Dhillon, W. Ullah, E. Keating, R. Providencia, A. Chow, M.J. Earley, R.J. Hunter, A novel mapping system for panoramic mapping of the left atrium: application to detect and characterize localized sources maintaining AF, JACC Clin. Electrophysiol. 4 (2018) 124–134.
[13] S. Honarbakhsh, R.J. Hunter, G. Dhillon, W. Ullah, E. Keating, R. Providencia, A. Chow, M.J. Earley, R.J. Schilling, Validation of a novel mapping system and utility for mapping complex atrial tachycardia, J. Cardiovasc. Electrophysiol. 29 (2018) 395–403.
[14] P. Sanders, J.B. Morton, N.C. Davidson, S.J. Spence, J.K. Vohra, P.B. Sparks, J.M. Kalman, Electrical remodelling of the atria in congestive heart failure: electrophysiological and electroanatomic mapping in humans, Circulation 108 (2003) 1461–1468.
[15] J.L. Harrison, H.K. Jensen, S.A. Peel, et al., Cardiac magnetic resonance and electroanatomical mapping of acute and chronic atrial ablation injury: a histological validation study, Eur. Heart J. 35 (2014) 1486–1495.
[16] S. Rolf, S. Kircher, A. Arya, C. Eitel, P. Sommer, S. Richter, T. Gaspar, A. Bollmann, D. Altmann, C. Piedra, G. Hindricks, C. Piorkowski, Tailored atrial substrate modification based on low-voltage areas in catheter ablation of atrial fibrillation, Circ. Arrhythm. Electrophysiol. 7 (2014) 825–833.
[17] S. Honarbakhsh, R.J. Schilling, R. Providencia, G. Dhillon, V. Sawhney, C.A. Martin, E. Keating, M. Finlay, S. Ahsan, A. Chow, M.J. Earley, R.J. Hunter, Panoramic atrial mapping with basket catheters: a quantitative analysis to optimize practice, patient selection and catheter choice, J. Cardiovasc. Electrophysiol. 28 (2017) 1423–1432.
[18] J. Laughner, S. Shome, N. Child, A. Shuros, P. Neuzil, J. Gill, M. Wright, Practical considerations of mapping persistent atrial fibrillation with whole-chamber basket catheters, JACC Clin. Electrophysiol. 2 (2016) 55–65.
[19] P. Jais, S. Matsuo, S. Knecht, R. Weerasooriya, M. Hocini, F. Sacher, M. Wright, I. Nault, N. Lellouche, G. Klein, J. Clementy, M. Haissaguerre, A deductive mapping strategy for atrial tachycardia following atrial fibrillation ablation: importance of localized re-entry, J. Cardiovasc. Electrophysiol. 20 (2009) 480–491.
[20] M.D. O'Neill, M. Wright, S. Knecht, et al., Long-term follow-up of persistent atrial fibrillation ablation using termination as a procedural endpoint, Eur. Heart J. 30 (2009) 1105–1120.
[21] S. Knecht, M. Sohal, I. Deisenhofer, et al., Multicentre evaluation of non-invasive biatrial mapping of persistent atrial fibrillation ablation: the AFACART study, Europace 19 (2017) 1302–1309.
[22] G. Yang, B. Yang, Y. Wei, et al., Catheter ablation of nonparoxysmal atrial fibrillation using electrophysiologically guided substrate modification during sinus rhythm after pulmonary vein isolation, Circ. Arrhythm. Electrophysiol. 9 (2016), e003382.
[23] A. Yagishita, J.R. Gimbel, S. DE Oliveira, H. Manyam, D. Sparano, I. Cakulev, J. Mackall, M. Arruda, Long-term outcome of left atrial voltage-guided substrate ablation during atrial fibrillation: a novel adjunctive ablation strategy, J. Cardiovasc. Electrophysiol. (2016), https://doi.org/10.1111/jce.13122.
[24] A.S. Jadidi, H. Lehrmann, C. Keyl, et al., Ablation of persistent atrial fibrillation targeting low-voltage areas with selective activation characteristics, Circ. Arrhythm. Electrophysiol. (2016), https://doi.org/10.1161/CIRCEP.115.002962.
[25] T. Baykaner, J.A.B. Zaman, A.J. Rogers, R. Navara, M. AlHusseini, R.T. Borne, S. Park, P.J. Wang, D.E. Krummen, W.H. Sauer, S.M. Narayan, Spatial relationship of sites for atrial fibrillation drivers and atrial tachycardia in patients with both arrhythmias, Int. J. Cardiol. 248 (2017) 188–195.
[26] S. Yamashita, D.A. Hooks, A. Shah, et al., Atrial tachycardias: cause or effect with ablation of persistent atrial fibrillation? J. Cardiovasc. Electrophysiol. 29 (2018) 274–283.
[27] G.M. Marcus, Y. Yang, P.D. Varosy, K. Ordovas, Z.H. Tseng, N. Badhwar, B.K. Lee, R.J. Lee, M.M. Schneiman, J.E. Olgin, Regional left atrial voltage in patients with atrial fibrillation, Heart Rhythm. 4 (2007) 138–144.
[28] R.J. Hunter, Y. Liu, Y. Lu, W. Wang, R.J. Schilling, Left atrial wall stress distribution and its relationship to electrophysiologic remodeling in persistent atrial fibrillation, Circ. Arrhythm. Electrophysiol. 5 (2012) 351–360.
[29] B. Burstein, P. Comtois, G. Michael, K. Nishida, L. Villeneuve, Y.H. Yeh, S. Nattel, Changes in connexin expression and the atrial fibrillation substrate in congestive heart failure, Circ. Res. 105 (2009) 1213–1222.
[30] Y. Xie, A. Garfinkel, P. Camelliti, P. Kohl, J.N. Weiss, Z. Qu, Effects of fibroblast-myocyte coupling on cardiac conduction and vulnerability to reentry: a computational study, Heart Rhythm. 6 (2009) 1641–1649.
[31] E.P. Gerstenfeld, D.J. Callans, W. Sauer, J. Jacobson, F.E. Marchlinski, Reentrant and non-reentrant focal left atrial tachycardia occurs after pulmonary vein isolation, Heart Rhythm. 2 (2005) 1195–2002.
[32] V. Markides, R.J. Schilling, S.Y. Ho, A.W. Chow, D.W. Davies, N.S. Peters, Characterization of left atrial activation in the intact human heart, Circulation 107 (2003) 733–739.
[33] F. Pashakhanloo, D. Herzka, H. Ashikaga, S. Mori, N. Gai, D.A. Bluemke, N.A. Trayanova, E.R. McVeigh, Myofiber architecture of the human atria as revealed by submillimeter diffusion tensor imaging, Circ. Arrhythm. Electrophysiol. 9 (2016), e004133, https://doi.org/10.1161/CIRCEP.116.004133.